

## Imaging and Spectroscopy of Single InAs Self-Assembled Quantum Dots using Ballistic Electron Emission Microscopy

M. E. Rubin,<sup>1</sup> G. Medeiros-Ribeiro,<sup>2</sup> J. J. O'Shea,<sup>2</sup> M. A. Chin,<sup>3</sup> E. Y. Lee,<sup>3</sup> P. M. Petroff,<sup>2</sup> and V. Narayanamurti<sup>3</sup>

<sup>1</sup>Physics Department, University of California, Santa Barbara, California 93106

<sup>2</sup>Materials Department, University of California, Santa Barbara, California 93106

<sup>3</sup>Electrical and Computer Engineering Department, University of California, Santa Barbara, California 93106

(Received 10 September 1996)

Single InAs self-assembled quantum dots buried spatially beneath a Au/GaAs interface are probed for the first time using the imaging and spectroscopic modes of ballistic electron emission microscopy (BEEM). BEEM images show enhanced current through each dot. Spectra taken with the tip positioned on a dot show shifted current thresholds when compared with the off dot spectra, which are essentially the same as those of Au on bulk GaAs. Shifts in the  $\Gamma$  and  $L$  conduction band thresholds are attributed to strain in the GaAs cap layer. Fine structure below the  $\Gamma$  threshold is consistent with resonant tunneling through zero-dimensional states within the quantum dots. [S0031-9007(96)01844-3]

PACS numbers: 73.20.Dx, 61.16.Ch

Quantum dots have generated a great deal of scientific and technological interest, exhibiting the effects of zero-dimensional (0D) confinement [1] and single electron charging [2]. Most of the measurements on these structures have required the use of sophisticated processing techniques and ultralow temperatures in order to resolve the small energy scales associated with these phenomena. Very recently, several groups have avoided these difficulties by using self-assembled quantum dots (SAD's), which are grown directly by molecular beam epitaxy (MBE) and are considerably smaller than those achievable by standard lithography [3]. Their small size ( $\sim 200$ – $300$  Å), however, makes contacting a single dot extremely difficult; therefore all previous electrical measurements have been on *ensembles* of hundreds or thousands of dots.

The study of the electrical transport through a *single* InAs SAD thus requires a technique with exceptional spatial resolution as well as spectroscopic capability. In this Letter we report the novel use of ballistic electron emission microscopy (BEEM) [4] to probe, with nanometer resolution, the transport through individual dots buried 50–75 Å below a metal-semiconductor interface. Our group has previously used BEEM to study electronic structure in nominally uniform, planar heterostructures with small lateral variations [5]. In a quantum dot, however, the electronic structure and thus the transport depend strongly on the specific local properties of that particular dot. Our measurements use the lateral scanning capability of BEEM to identify and probe dots one at a time, and demonstrate the power of BEEM as a tool for studying local transport through, and spectroscopy of, *individual* localized semiconductor quantum structures.

It is well known that under certain conditions self-assembled InAs quantum dots can be grown within a GaAs matrix, and that these dots are  $\sim 300$  Å in diameter and  $\sim 30$  Å high [3]. For the BEEM experiment, the dots were grown on top of a 300 Å undoped GaAs buffer

layer which itself was grown on a conducting  $n^+$  GaAs substrate. Another undoped GaAs layer, either 50, 65, or 75 Å thick, was grown on top of the dots, and an 85 Å Au layer was evaporated *ex situ* on top of this layer, forming the Schottky barrier necessary for BEEM. The two GaAs layers have a wider band gap than the InAs so that electrons may be confined within the dot in all three spatial directions, which is, in fact, the defining condition for a quantum dot.

Figure 1 shows the situation when the scanning tunneling microscope (STM) tip is positioned at and away from a single InAs dot, respectively (i.e., *on* and *off* the dot). Away from the dots there is only a thin InAs wetting layer ( $\sim 1.5$  monolayer thick) [3] which has little effect on the potential. BEEM current images and spectra for this case are therefore very similar to those for the planar Au/GaAs interface, which has been studied extensively [4,5]. When the tip is above a dot, however, the local transport properties of the dot and surrounding material strongly affect the BEEM measurements.

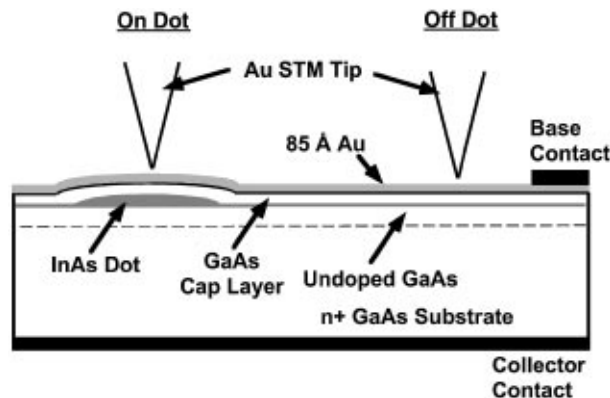


FIG. 1. Schematic cross-sectional views of the sample structure for the STM tip positioned on and off a quantum dot.

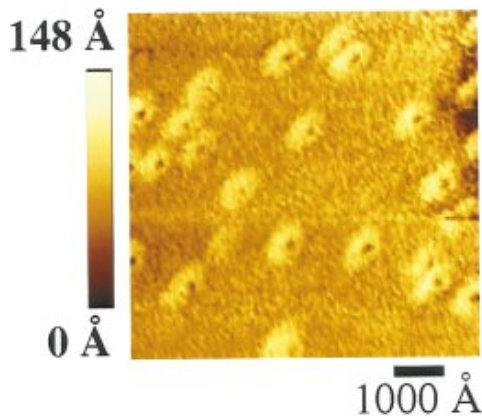


FIG. 2(color). STM image of surface features in a region where several InAs quantum dots are present and capped with a 50 Å GaAs layer and 85 Å Au layer. The dips near the center of each feature represent the positions of the dots beneath the surface.

The STM imaging mode of the BEEM microscope was used to spatially locate the dots. Figure 2 shows a  $7500 \text{ \AA} \times 7500 \text{ \AA}$  STM image taken with a 1 nA tunnel current which shows the surface features above several dots covered by a 50 Å GaAs cap layer and 85 Å Au layer. The features are  $\sim 1000 \text{ \AA}$  in diameter and 30–50 Å high. Au grains, with diameter  $\sim 200 \text{ \AA}$ , are also visible. An immediately obvious characteristic in this image is the dip near the center of each feature. These dips, which had not previously been directly observed, are very repeatable and have lateral dimensions of  $\sim 300 \text{ \AA}$ . Because they are also present in atomic force microscopy (AFM) images of the surface, with and without the Au layer present, they are not an artifact of the tips (STM or AFM) or caused by the metallization process.

A simple explanation for the presence of these dips is that the lattice mismatch between the InAs dots and the GaAs cap layer causes a preferential buildup of GaAs away from the center of the dot during the growth process. The strain in the InAs dots is relaxed such that the top center of the dots have a lattice constant closer to that of unstrained InAs, while the edges of the dot, being nearer the pseudomorphic wetting layer, have lattice constant more like that of unstrained GaAs. The overgrown GaAs therefore prefers to fit into sites away from the center of the dot. Furthermore, in order for the cap layer to fit onto the wider lattice constant dot it must undergo tensile biaxial strain, which would tend to thin the layer in the growth direction. A cap layer grown nominally thicker should result in a less prominent dip, and this was in fact observed. TEM studies of the strain in InAs SAD's support this model [6].

Figure 3(a) shows a higher resolution room temperature STM image of the surface above a *single* InAs quantum dot, capped with a 75 Å GaAs layer. Both the dip and the Au grains can still be seen clearly; in fact, Au grains

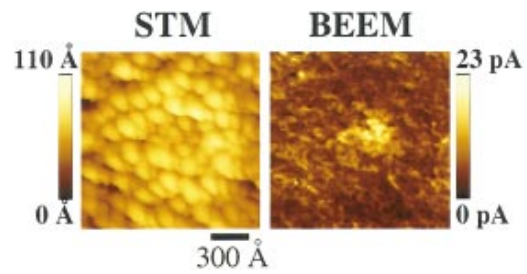


FIG. 3(color). Simultaneously measured STM and BEEM images of a *single* InAs dot capped with 75 Å GaAs buried beneath the surface. The dip and Au grains are visible in the STM image, and a strong enhancement of the BEEM current is present at the position of the dip.

can be resolved within the dip, which is  $\sim 25\text{--}30 \text{ \AA}$  deep. This depth implies that the GaAs cap layer is at most 40–50 Å thick above the dot for this case. Figure 3(b) is the concurrently measured BEEM image, which was scanned with a tunnel current of 2 nA and a bias voltage of 1.5 V, well above the Schottky barrier height. A strong enhancement of the BEEM current is present in the area of the dip, where the quantum dot is buried beneath the surface. An enhanced BEEM current generally implies a lowered initial threshold, which is consistent with the model of a strained cap layer above the dot, since tensile biaxial strain in GaAs tends to lower the conduction band edges [7].

More quantitative information can be discerned from BEEM spectra. Figure 4 shows the averages of at least one thousand voltage scans for each curve taken at room temperature on and off of a single dot capped with 75 Å GaAs, using a 4 nA tunnel current. These data are representative of that seen on several dots which all showed qualitatively similar features. Away from the dot, the solid curve shows a two valley Bell-Kaiser model [4,8] least squares fit to the data which yields an initial  $\Gamma$  threshold of 0.85 V and a  $L$  valley threshold of 1.20 V, marked with arrows. These are

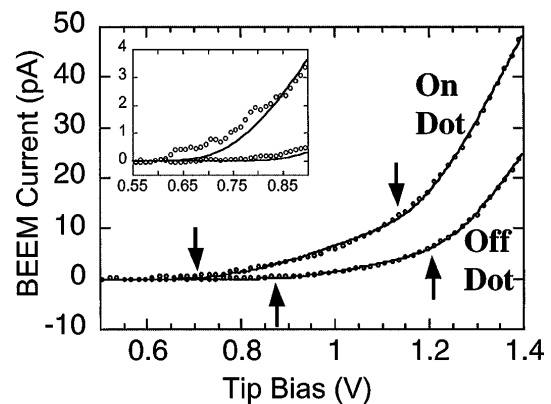


FIG. 4. BEEM spectra on and off the dot, showing shifts in thresholds and structure on the dot at energies below the Schottky barrier threshold due to 0D resonant tunneling.

approximately the accepted values for the planar, uniform Au/GaAs interface [5,9].

Although the Bell-Kaiser model does not account for the presence of the quantum dot, a fit to the on dot spectrum is also shown as a solid curve in Fig. 4. Clearly the curve is a poor fit to the data, especially close to the lowest threshold, as can be seen in the inset of Fig. 4 which shows an expanded view of the same data as the main curves. With this caveat in mind, we note that the fit yields a  $\Gamma$  threshold at 0.69 V and an  $L$  threshold at 1.14 V, corresponding to downward shifts, between the off and on dot cases, of 0.16 and 0.06 V for the  $\Gamma$  and  $L$  valley conduction band edges, respectively.

The shifts in the conduction band edges in GaAs are dominated by the hydrostatic component of the strain, assuming that the shear components of the strain are small [10]. The shifts are  $\delta E_c^{\Gamma,L} = a_c^{\Gamma,L}(\varepsilon_{xx} + \varepsilon_{yy} + \varepsilon_{zz})$ , where  $a_c^{\Gamma,L}$  are the deformation potentials for the  $\Gamma$  and  $L$  conduction bands, respectively, and  $\varepsilon_{xx}$ ,  $\varepsilon_{yy}$ , and  $\varepsilon_{zz}$  are the diagonal strain components. Thus the ratio of shifts for these bands is independent of the particular strain. For GaAs,  $(\delta E_c^{\Gamma}/\delta E_c^L) \approx a_c^{\Gamma}/a_c^L \approx -15.93/-11.49 \approx 1.4$  [11]. The shifts in the measured BEEM thresholds, as determined by the Bell-Kaiser fit, however, have a ratio of  $\approx 2.7$ . Inspection of the inset to Fig. 4 resolves this discrepancy. Near the initial threshold of the on dot curve, additional fine structure increases the BEEM current relative to that predicted by the model, causing the fit to yield a  $\Gamma$  threshold that is artificially low. The  $L$  threshold should be relatively unaffected by the fine structure, however, so the above ratio can be used with the measured  $L$  shift to predict a strain induced  $\Gamma$  shift of  $\approx 0.08$  eV, placing the barrier height closer to  $\sim 0.77$  eV.

Within this picture, most of the fine structure lies energetically *below* the Schottky barrier. This is very different than traditional BEEM, where current flow begins only when carriers are injected above this barrier. Another mechanism, directly related to the presence of the quantum dot, must therefore account for this extra current. The spectrum has two main features beginning at  $\sim 0.62$  and  $\sim 0.72$  V, respectively. In both cases, the current initially rises, then tends to bend towards zero slope. This behavior is consistent with resonant tunneling into 0D states within the quantum dot.

Figure 5 schematically shows the potential along a line in the growth direction from the STM tip through the base and a quantum dot. As is clear from the diagram, band bending near the Au/GaAs interface creates a localized double barrier structure where the dot acts as the well region between the barriers. The dot is confined in all three spatial directions, so 0D states can exist within the dot. Away from the dot, where there is only the thin wetting layer, the potential is essentially a wide, triangular, single barrier, and no confinement occurs.

The BEEM current due to resonant tunneling below the Schottky barrier can be described as a convolution between

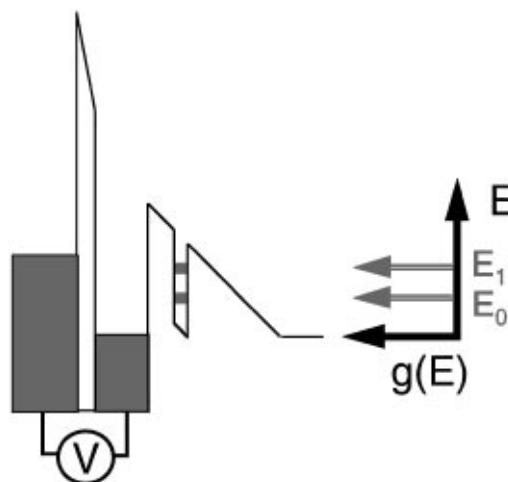


FIG. 5. Schematic potential profile along a line through a quantum dot. Band bending creates a double barrier structure with 0D states confined within the dot.

the electron distribution in the base and the density of states  $g(E)$  in the dot. For the range of energies and tip biases which contribute to the fine structure, the electron distribution can be assumed to be roughly constant [4]. If  $g(E)$  is taken to be the delta function density of states for a 0D system, then the convolution (at 0 K) is a series of steps, with each leading edge occurring at the energy of a state. Note that the metallic nature of the STM tip emitter in the BEEM case leads to different behavior than in traditional semiconductor emitter resonant tunneling diodes.

Allowing for broadening due to finite temperature, the on dot data is described by this model reasonably well. The two features in the fine structure imply tunneling through two 0D states, separated by  $\sim 0.1$  eV. Because the position of the conduction band edge in the dot is not known with respect to the base Fermi energy, the absolute energies of the states cannot be measured with this technique; however, the presence of two states separated by  $\sim 0.1$  eV agrees with theoretical calculations [12]. Capacitance spectroscopy of ensembles of dots show somewhat smaller separations ( $\sim 0.05$  eV) in a different sample geometry [13,14]. In our case, the strong band bending causes a large electric field through the dot, which tends to increase the energy separation of the states.

In summary, we have provided the first evidence of local electrical transport through a single self-assembled InAs quantum dot, using BEEM. The measured current spectra exhibit gross effects which are consistent with strain induced shifts of the conduction band edges of the cap layer, and fine structure consistent with resonant tunneling through two 0D states in the dot. The images clearly show the power of BEEM to spatially localize lateral energetic features in individual, nanometer scale, semiconductor quantum structures buried beneath the surface. We will exploit this technique to perform further studies of

these and other structures with varying temperature, externally applied bias, and magnetic field. Such detailed studies should lead to both a fundamental understanding of the physics of lower dimensional structures and their technological applications.

We thank Dr. D.L. Smith (Los Alamos National Laboratory) for extensive discussions, and E. Brazel and S. Bhargava for useful discussions. This work was supported by AFOSR Grant No. 442530-22502 and NSF National Science and Technology Center for Quantized Electronic Structures (QUEST) Grant No. DMR91-20007.

- 
- [1] For example, M.A. Reed, J.N. Randall, R.J. Aggarwal, R.J. Matyi, T.M. Moore, and A.E. Wetsel, *Phys. Rev. Lett.* **60**, 535 (1988).
- [2] For example, R.C. Ashoori, H.L. Stormer, J.S. Weiner, L.N. Pfeiffer, S.J. Pearton, K.W. Baldwin, and K.W. West, *Phys. Rev. Lett.* **68**, 3088 (1992).
- [3] For example, D. Leonard, M. Krishnamurthy, C.M. Reaves, S.P. Denbaars, and P.M. Petroff, *Appl. Phys. Lett.* **63**, 3203 (1993).
- [4] L.D. Bell and W.J. Kaiser, *Annu. Rev. Mater. Sci.* **26**, 189 (1996), and references therein; M. Prietsch, *Phys. Rep.* **253**, 163 (1995), and references therein.
- [5] J.J. O'Shea, T. Sajoto, S. Bhargava, D. Leonard, M.A. Chin, and V. Narayanamurti, *J. Vac. Sci. Technol. B* **12**, 2625 (1994); T. Sajoto, J.J. O'Shea, S. Bhargava, D. Leonard, M.A. Chin, and V. Narayanamurti, *Phys. Rev. Lett.* **74**, 3427 (1995).
- [6] Q. Xie, P. Chen, and A. Madhukar, *Appl. Phys. Lett.* **65**, 2051 (1994).
- [7] C. Van de Walle, *Phys. Rev. B* **39**, 1871 (1989).
- [8] The exact values for BEEM current thresholds are model dependent, and therefore should only be considered relative to other values found using the same fit. We use the Bell-Kaiser model to consistently compare new results with previous work, although it may not account for all relevant parameters.
- [9] The slightly higher  $\Gamma$  thresholds reported in Refs. [4,5] were for different sample geometries, where different image potential lowerings and doping profiles affect the threshold.
- [10] M. Grundmann, O. Stier, and D. Bimberg, *Phys. Rev. B* **52**, 11 969 (1995).
- [11] M. Cardona and N.E. Christensen, *Phys. Rev. B* **35**, 6182 (1987).
- [12] J.-Y. Marzin and G. Bastard, *Solid State Commun.* **92**, 437 (1994).
- [13] H. Drexler, D. Leonard, W. Hansen, J.P. Kotthaus, and P.M. Petroff, *Phys. Rev. Lett.* **73**, 2252 (1994); G. Medeiros-Ribeiro, D. Leonard, and P.M. Petroff, *Appl. Phys. Lett.* **66**, 1767 (1995).
- [14] K. Schmidt, G. Medeiros-Ribeiro, M. Ostereich, and P.M. Petroff, *Phys. Rev. B* (to be published).